LEVEL II

GENERAL ⬤ ELECTRIC

MILITARY ELECTRONIC SYSTEMS OPERATION

TECHNICAL INFORMATION SERIES

AD A092968

Author	Subject Category	No. R80EMH8
John P. Costas	Spectral Analysis	Date October 1980

Title RESIDUAL SIGNAL ANALYSIS - A SEARCH AND DESTROY APPROACH TO SPECTRAL ANALYSIS.

Copies Available at MESO TIS Distribution Center Box 4840 (CSP 4-18) Syracuse, New York 13221	GE Class 1	No. of Pages
	Govt Class Unclassified	36

Summary

A signal processing procedure especially suited for use in narrowband spectral analysis or "line tracking" applications is presented. A modular approach is used which permits each tracker to optimize estimation parameters for the line assigned. The signal estimate from each module is used to cancel the corresponding signal from the common bus to which all tracker inputs are connected. A feedback arrangement around each module restores full level to each tracker of its own assigned input signal. Each signal being tracked is thus prevented from causing interference to any other tracker. The advantages are obtained from this arrangement are demonstrated and discussed.

DTIC
ELECTE
DEC 17 1980
E

DDC FILE COPY

4/11962

Send to_____

GENERAL ELECTRIC COMPANY TECHNICAL INFORMATION

Within the limitations imposed by Government data export regulations and security classifications, the availability of General Electric Company technical information is regulated by the following classifications in order to safeguard proprietary information:

CLASS 1: <u>GENERAL INFORMATION</u>

Available to anyone on request.
Patent, legal and commercial review
required before issue.

CLASS 2: <u>GENERAL COMPANY INFORMATION</u>

Available to any General Electric Company
employee on request.
Available to any General Electric Subsidiary
or Licensee subject to existing agreements.
Disclosure outside General Electric Company
requires approval of originating component.

CLASS 3: <u>LIMITED AVAILABILITY INFORMATION</u>

Original Distribution to those individuals with
specific need for information.
Subsequent Company availability requires
originating component approval.
Disclosure outside General Electric Company
requires approval of originating component.

CLASS 4: <u>HIGHLY RESTRICTED DISTRIBUTION</u>

Original distribution to those individuals person-
ally responsible for the Company's interests in
the subject.
Copies serially numbered, assigned and recorded
by name.
Material content, and knowledge of existence,
restricted to copy holder.

GOVERNMENT SECURITY CLASSIFICATIONS, when required, take precedence in the handling of the material. Wherever not specifically disallowed, the General Electric classifications should also be included in order to obtain proper handling routines.

GENERAL ELECTRIC COMPANY
MILITARY ELECTRONIC SYSTEMS OPERATIONS
TECHNICAL INFORMATION SERIES

SECTION ___ Advanced Technical Programs

UNIT ___ 570

MESO ACCOUNTING REFERENCE ___ 570

COLLABORATORS ___

APPROVED ___ J.J. Gostin ___ TITLE Manager, ATP LOCATION ___ CSP 4-58

MINIMUM DISTRIBUTION - Government Unclassified Material (and Title Pages) in G.E. Classes 1, 2, or 3 will be the following.

Copies	Title Page Only	To
0	1	Legal Section, MESO (Syracuse)
0	1	Manager, Technological Planning, MESO (Syracuse)
5	6	G-E Technical Data Center (Schenectady)

MINIMUM DISTRIBUTION - Government Classified Material, Secret or Confidential in G.E. Classes 1, 2, or 3 will be the following.

1	0	Manager, Technological Planning, MESO (Syracuse)

ADDITIONAL DISTRIBUTION (Keep at minimum within intent of assigned G.E. Class.)

COPIES	NAME	LOCATION
5 (CLASS 1 ONLY)	DEFENSE DOCUMENTATION CENTER	CAMERON STATION, ALEXANDRIA, VA. 22314
1	L. I. Chasen	P.O. Box 8555 Philadelphia, Pa., 19101
1	W. B. Adams	CSP 4-57, Syracuse, NY 13221
1	A. A. Albanese	CSP 4-57, Syracuse, NY 13221
1	S. P. Applebaum	CSP 4-38A, Syracuse, NY 13221
1	L. W. Bauer	Bldg 57 - Rm 525, Schenectady, NY
1	D. R. Bonewell	FRP 1-6D, Syracuse, NY 13221
1	E. K. Chin	CSP 4-4, Syracuse, NY 13221
1	D. B. Connolly	CSP 4-57, Syracuse, NY 13221
1	F. M. DeBritz	FRP 1-6D, Syracuse, NY 13221
1	F. R. Dickey	CSP 4-38A, Syracuse, NY 13221
1	J. P. Dietz	FRP 1-4J, Syracuse, NY 13221
1	L. O. Eber	CSP 4-3, Syracuse, NY 13221
1	J. A. Edward	CSP 4-48, Syracuse, NY 13221
1	D. B. Friedman	CSP 4-49, Syracuse, NY 13221
1	V. T. Gabriel	FRP 1-6D, Syracuse, NY 13221
1	S. M. Garber	CSP 4-48, Syracuse, NY 13221
1	E. P. Gasparek	CSP 4-57, Syracuse, NY 13221
1	J. J. Gostin	CSP 4-58, Syracuse, NY 13221
1	R. E. Hansen	FRP 1-6D, Syracuse, NY 13221
1	R. L. Herman	FRP 2-31, Syracuse, NY 13221
1	H. L. Hodgskin	FRP 1-4B, Syracuse, NY 13221

80 12 15 008

Additional Distribution (Cont)

Copies	Name	Location
1	W. C. Hollis	FRP 1-M6, Syracuse, NY 13221
1	N. A. Hoy	FRP 1-M8, Syracuse, NY 13221
1	C. P. Hsieh	CSP 4-5, Syracuse, NY 13221
1	M. Hunter	French Rd, MD 289 Utica, NY
1	M. H. Hutchison	FRP 1-N1, Syracuse, NY 13221
1	R. V. Jackson	CSP 4-5, Syracuse, NY 13221
1	M. A. Johnson	CSP 4-58, Syracuse, NY 13221
1	R. R. Kinsey	CSP 4-57, Syracuse, NY 13221
1	D. Kittleson	FRP 1-M6, Syracuse, NY 13221
1	L. Knickerbocker	FRP 1-N1, Syracuse, NY 13221
1	D. H. Kuhn	CSP 4-57, Syracuse, NY 13221
1	J. P. Kuhn	CSP 4-48, Syracuse, NY 13221
1	L. R. Lemon	FRP 1-4C, Syracuse, NY 13221
1	J. P. Lindhuber	CSP 4-48, Syracuse, NY 13221
1	J. R. Loeffler	FRP 1-M4, Syracuse, NY 13221
1	J. F. Lomber	FRP 1-J7, Syracuse, NY 13221
1	M. B. McGuinness	FRP 1-N1, Syracuse, NY 13221
1	T. McJilton	CSP 4-49, Syracuse, NY 13221
1	J. H. McMaster	FRP 1-6D, Syracuse, NY 13221
1	J. F. McNeill	FRP 1-6B, Syracuse, NY 13221
1	C. S. Monz	FRP 1-4M, Syracuse, NY 13221
1	V. Nasipak	FRP 2-31, Syracuse, NY 13221
1	C. E. Nelson	CSP 4-38A, Syracuse, NY 13221
1	R. Nitzberg	CSP 4-5, Syracuse, NY 13221
1	R. J. Nosenzo	CSP B, Syracuse, NY 13221
1	G. Oehling	CSP 4-5, Syracuse, NY 13221
1	K. A. Olsen	CSP 4-5, Syracuse, NY 13221
1	J. R. Olson	FRP 1-6A, Syracuse, NY 13221
1	P. E. Pedley	FRP 1-9D, Syracuse, NY 13221
1	E. H. Peterson	FRP 1-6D, Syracuse, NY 13221
1	J. R. Pratt	CSP 4-5, Syracuse, NY 13221
1	A. J. Rasi	FRP 1-5F, Syracuse, NY 13221
1	F. G. Recny	CSP C, Syracuse, NY 13221
1	J. G. Reddeck	CSP 4-5, Syracuse, NY 13221
1	J. A. Rougas	CSP 4-4, Syracuse, NY 13221
1	E. Shain	FRP 1-B4, Syracuse, NY 13221
1	F. D. Shapiro	CSP 4-5, Syracuse, NY 13221
1	O. H. Shuart	CSP 4-38A, Syracuse, NY 13221
1	J. Slocum	CSP 4-4, Syracuse, NY 13221
1	F. G. Spann	FRP 1-6D, Syracuse, NY 13221
1	M. T. Stark	CSP 4-48, Syracuse, NY 13221
1	J. W. Stauffer	CSP 4-48, Syracuse, NY 13221
1	C. A. Stutt	Bldg 5 - Rm 209 Schenectady, NY
1	R. F. Sweetman	FRP 1-6D, Syracuse, NY 13221

Additional Distribution (Cont)

Copies	Name	Location
1	R. J. Talham	FRP 1-A5, Syracuse, NY 13221
1	R. M. Teza	FRP 1-4J, Syracuse, NY 13221
1	M. Viggiano	CSP 4-57, Syracuse, NY 13221
1	B. P. Viglietta	CSP 4-57, Syracuse, NY 13221
1	A. M. Vural	CSP 4-58, Syracuse, NY 13221
1	L. Waful	FRP 1-N1, Syracuse, NY 13221
1	R. Wasiewicz	CSP 4-5, Syracuse, NY 13221
1	W. C. Webster	FRP 1-6D, Syracuse, NY 13221
1	W. Whyland	CSP 4-48, Syracuse, NY 13221
1	D. W. Winfield	CSP 4-48, Syracuse, NY 13221

Accession For

NTIS GRA&I ☒
DDC TAB ☐
Unannounced ☐
Justification_____

By_____
Distribution/
Availability Codes

Dist	Avail and/or special
A	

TABLE OF CONTENTS

LIST OF ILLUSTRATIONS

GLOSSARY

C PA	Closest Point of Approach
CW	Continuous Wave
dB	Decibel
FFT	Fast-Fourier Transform
FDL	Frequency Discriminator Loop
ISB	Input Signal Bus
mHz	Millihertz
MHz	Megahertz
PLL	Phase-Locked Loop
RSA	Residual Signal Analysis
RSB	Residual Signal Bus
s	Second
SNR	Signal-to-Noise Ratio
TCU	Tracker Control Unit
TSB	Tracker Signal Bus

SECTION I

INTRODUCTION

Spectral analysis procedures of various kinds are often applied to what may be loosely called the "line-tracking" problem. If a signal component of interest is described as a "line", this implies a confined or "narrow" spectral width. Such descriptors are relative and somewhat vague. I remember well the airline captain who reassured a nervous fellow passenger before takeoff in the bygone piston/propeller era that all of his flights were smooth --- but that some flights were smoother than others. In a corresponding fashion all of the line signals of interest here are narrow with some lines being much narrower than others. In spite of the imprecision of definition, the line tracking operation may be considered as one in which the parameters of signals qualifying as "lines" are to be determined and kept updated. Such parameters may include center frequency, spectral width or shape, mean power level, and relative phase.

A well-known class of trackers involves comb filtering in the frequency domain provided by processors such as fast-Fourier transforms (FFT's). The individual comb signals are detected and the ensemble of detected outputs is presented to associative processors which sense contiguous amplitude anomalies in the frequency-time space and declare a "track" condition depending on program specifications. Various visual presentations of temporal spectral-level (e.g. lofargrams) data have also been used with good success to provide a line detection and tracking capability.

The wide variety of line trackers which exist and others which are currently under development give some indication of the importance of these techniques and of the failure of a "universal" technique to emerge. Some of the difficulties of the comb filter, postdetector processor/tracker approach, for example, are worthy of a short discussion. The use of an up-front coherent processor such as an FFT for all lines requires that the frequency resolution choice be a compromise. Some lines will span many FFT cells while others may occupy a very small part of a single frequency resolution cell. In the former case special post-detection processor logic will be required in order that the signal smear (relative to the spectrum analyzer) may be recognized as a line. In the latter case the potential of the line in terms of detection level and frequency or phase determination is squandered by an obviously inadequate processor. The compromise frequency resolution choice for the head-end FFT is seldom a satisfactory one since line widths encountered in may practical applications can vary by several orders of magnitude.

In some situations many of the lines present are of no real interest except for possible anomalous behavior. Once these lines are detected and identified, one only wishes to be made aware of an unusual event such as the sudden disappearance of one or more of these lines. During routine periods such lines act really as jammers, cluttering up displays and interfering with signal processing operations on other, often much weaker signals which may be of primary interest. The frequency-quantization property of comb filters such as the FFT is one of the prices paid for economy in spectral computation. In the tracking operation such compartmentization by frequency can be troublesome since a line signal will often move through several frequency cells in the course of an analysis. Computation of line frequency and relative phase can also be complicated by the combination of a signal which exists in a frequency continuum and an analysis procedure which imposes the nuisance of frequency quantization.

The nature of the line tracking problem varies greatly with specific application. The residual signal analysis (RSA) procedure presented here is a technique which has some unique and very useful properties. In some applications the RSA subsystem can satisfy the entire line tracking requirement. In other cases these algorithms can work best as a preprocessor ahead of existing spectral analysis systems.

1. BASIC PRINCIPLES

Operation of the residual signal analysis (RSA) system will now be described with reference to Figure 1-1. Both time and level quantization are assumed in the descriptions which follow. Three main signal lines or buses are used: the Input Signal Bus (ISB), the Tracker Signal Bus (TSB) and the Residual Signal Bus (RSB). Discrete processing entities called tracker modules (TM_r) are made available and are assigned exclusively to each line being tracked. These processing entities may be instrumented in hardware, software or in combination. The methodology internal to the tracker modules can be of various types which will be described and discussed later.

For the moment it is sufficient to understand that a tracker module is assigned to one spectral line only. The module contains logic which senses that the assigned line has indeed been "acquired" so that an internal "track" flag may be set true. An external switch S_r is closed only when "track" is true, otherwise the switch is open and that module makes no contribution to the Tracker Signal Bus

Once track is achieved the tracker module optimizes its operating parameters to match the spectral width and dynamics of the assigned line. After each clock cycle the tracker module provides at its output an estimate of the signal value which will exist at the next clock or sampling time. This predicted signal voltage estimate is delayed (saved) for one

1-2

clock or sampling time. This predicted signal voltage estimate is saved so that it will be immediately available at the next clock cycle.
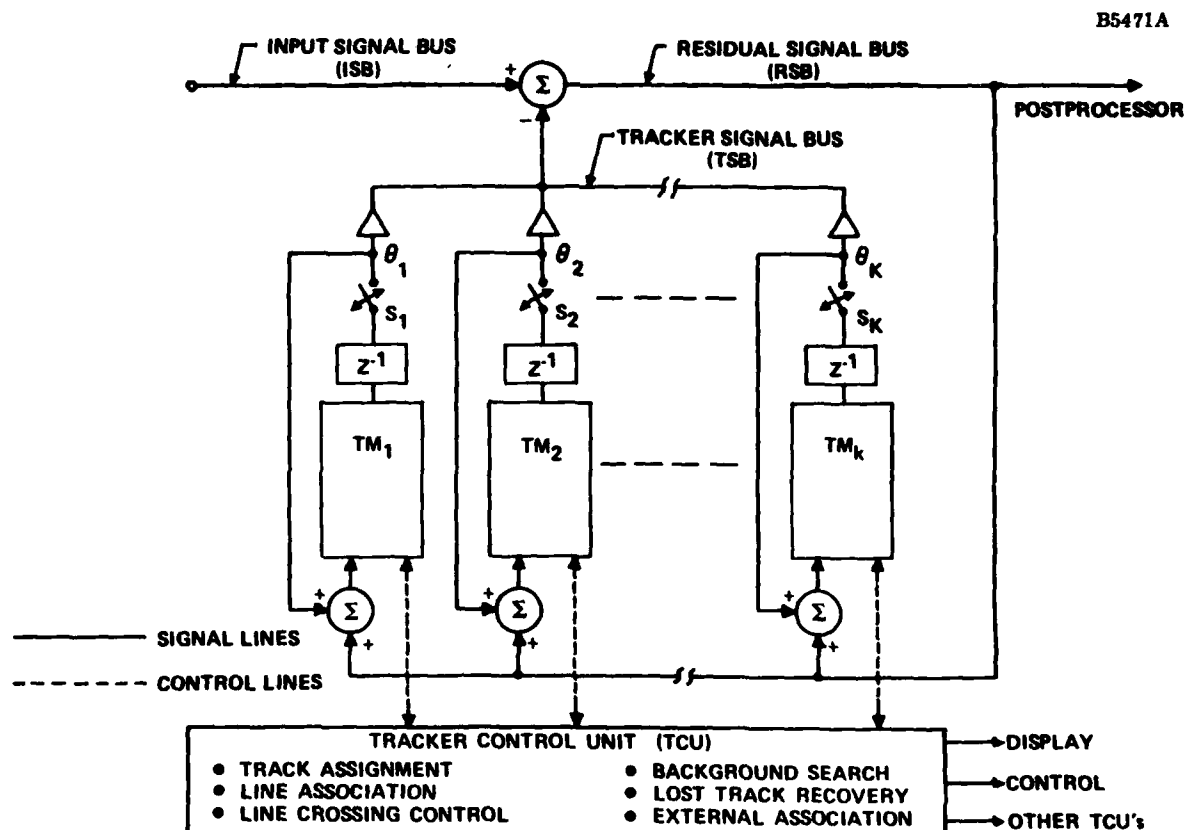
B5471A

Figure 1-1. Residual Signal Analysis (RSA) System Block Diagram

At the next sampling time the Input Signal Bus voltage has subtracted from it the Tracker Signal Bus voltage which contains the sum of signal estimates of operative trackers. The difference voltage is placed on the Residual Signal Bus, which, if all has gone well, contains greatly attenuated a versions of the signals being tracked. This Residual Signal Bus voltage feeds the postprocessing subsystems (if any) and also feeds each of the trackers.

At this point we have a bit of a problem. If the trackers are doing a good job then there will be only vestiges of the input spectral line signals on the Residual Signal Bus which forms the common drive to the trackers. There will, in fact, be very little in the way of lines for the trackers to track. If track is lost, the switches S_r open, the Input Signal Bus voltage and the Residual Signal Bus voltage become identical and the spectral lines reappear at the tracker inputs.

In order to resolve this difficulty, feedback is provided around each tracker module. This at first appears to be positive feedback but in fact, it is not. Note in Figure 1-1 that tracker module 1, for example, contributes a voltage θ_1 to the Tracker Signal Bus (track condition assumed, switch S_1 closed). This voltage component when subtracted from the Input Signal Bus voltage eliminates the spectral line being tracked by module 1 from appearing on the Residual Signal Bus. If this voltage θ_1, is added back to the Residual Signal Bus voltage to form the actual input or drive to tracker module 1, as shown, then there is in fact no feedback around the module. Note also that the spectral line being tracked by module 1 appears unaltered at the input to that module but does not appear at any other module input because of it's (relative) absence from the Residual Signal Bus.

If this argument is extended to include simultaneous operation of a number of trackers, it may be seen that each tracker sees its own signal unattenuated. However, each tracked signal is (nearly) transparent to all of the other trackers or other processors (such as displays) that may be fed from the Residual Signal Bus. The system is thus "failsafe" in the sense that a signal line lost or dropped from track by an assigned module, appears at once on the Residual Signal Bus. Generally speaking lines not seen on the Residual Signal Bus are lines already accounted for by the tracker module processors. The Residual Signal Bus contains at all times those signals which remain after tracker-module processing and are "residual" to this process.

Physical signal elimination has many advantages, some of which are not obvious at first glance. Consider the original line acquisition problem relative to Figure 1-1. The tracker control unit (TCU) dispatches the first tracker (Say TM_1) to search for and acquire a spectral line within a specified passband. Once this tracker indicates acquisition to the TCU a second tracker (Say TM_2) may be dispatched. Since the line already being tracked by TM_1 is transparent to the searching TM_2, this second tracker will usually pass by the spectral line already acquired, and lock on to a spectral line beyond this point. Upon receipt of a lock signal from TM_2, TM_3 is dispatched, and so forth. The "search and destroy" nature of this procedure can thus be used to good advantage in the initialization process.

A spectral line parameter of routine interest is line "center" frequency. Such frequency estimates can be badly biased by the presence of strong lines in the frequency neighborhood of the spectral line of real interest. While measurement means can be devised which attenuate off-frequency signals over extended skirt frequency regions, such approaches tend to be expensive. In the RSA system a line tracked is a line eliminated and this normally represents an inexpensive means for getting (effectively) skirt attenuation at precisely those frequency locations where attenuation is needed. Generally speaking, a strong line should be tracked even if it is of no interest since it can interfere with the processing of other lines.

1-4

The reduction of dynamic range by strong line elimination through RSA acquisition can be very useful. This is especially true when limited amplitude tolerance is encountered in a subsystem such as an amplitude-frequency-time display. Much new information can often be seen on such displays in the region of a strong line, once that line has been RSA-removed. In fact the man-machine process can be iterative. Lines observed are removed by operator module assignments. Once this is done, display levels may be readjusted to reveal new lines which in turn may be given special RSA attention. The property that the operator sees only what the hardware is not accounting for provides for some very useful man-machine team characteristics.

The above qualitative discussion has presented the basic principles of the RSA technique and has allowed some of the advantages of this approach to be indicated. In the following sections some simple quantitative results are obtained and some comparisons of tracker module implementation schemes are given.

SECTION II

ANALYTICAL DETAILS

A simple analysis of tracker module operation will now be given with the aid of Figure 2-1. It is assumed that there are K-operative modules and only the rth module is shown in Figure 2-1. A linear operator $H_r(Z)$ is assumed as the processor of the module drive signal $d_{r,n}$ to produce the signal $\theta_{r,n}$ which is an estimate of the rth spectral line voltage as it will appear at the next sampling time index $(n + 1)$. Specific implementations of the module linear operator $H_r(Z)$ will be discussed later. For the present the general representation indicated in Figure 2-1 is appropriate.
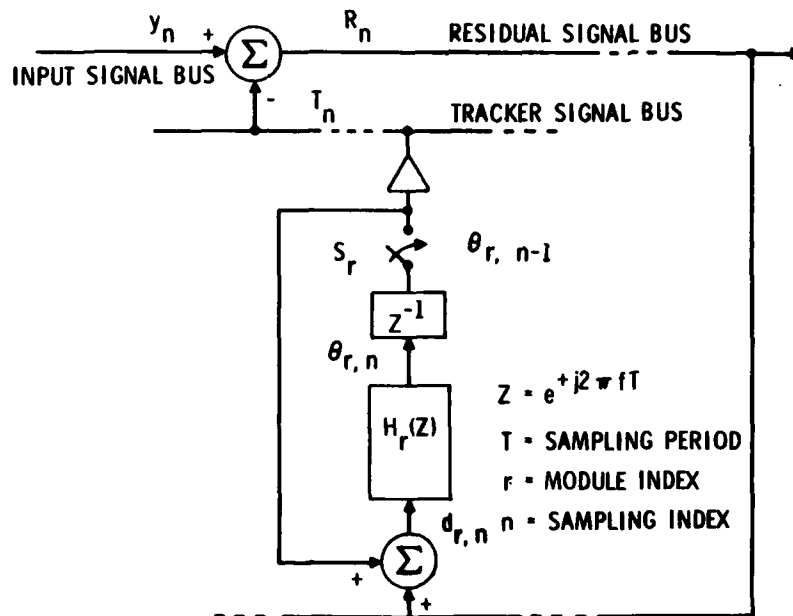

Figure 2-1. Tracker Module Details

The algebra of Figure 2-1 follows easily. The residual signal is the difference between input signal and Tracker Signal Bus value

$$R_n = y_n - T_n \tag{2-1}$$

The rth module drive signal is

$$d_{r,n} = R_n + \theta_{r,\,n-1} \ .$$ (2-2)

The Tracker Signal Bus voltage is the sum

$$T_n = \sum_{k=1}^{K} \theta_{k,\,n-1}$$ (2-3)

Combining Equations (2-1), (2-2), and (2-3) gives

$$d_{r,n} = y_n - \sum_{k=1}^{K} \theta_{k,\,n-1} + \theta_{r,\,n-1}$$ (2-4)

which may be written as

$$d_{r,n} = y_n - \sum_{\substack{k=1 \\ k \neq r}}^{K} \theta_{k,\,n-1}$$ (2-5)

Equation (2-5) demonstrates the basic concept of the RSA technique. The input to a module assigned to a specific spectral line signal is the subsystem input signal less the estimates of all other spectral line signals being tracked.

Taking Z-transforms of Equations (2-1), (2-2), and (2-3) yields, respectively

$$R(Z) = Y(Z) - T(Z)$$ (2-6)

$$D_r(Z) = R(Z) + Z^{-1} \theta_r(Z)$$ (2-7)

$$T(Z) = \sum_{k=1}^{K} Z^{-1} \theta_k(Z) \ .$$ (2-8)

Figure 2-1 provides the immediate result

$$\theta_r(Z) = H_r(Z) \cdot D_r(Z) \ .$$ (2-9)

Equation (2-6) yields

$$G(Z) \triangleq \frac{R(Z)}{Y(Z)} = \frac{1}{1 + \frac{T(Z)}{R(Z)}} \qquad (2\text{-}10)$$

where $G(Z)$, as defined here, becomes the transfer function of the RSA subsystem. Equations (2-7) and (2-9) combine to give

$$\frac{\theta_r(Z)}{R(Z)} = \frac{H_r(Z)}{1 - Z^{-1} H_r(Z)} \qquad (2\text{-}11)$$

which when substituted into Equation (2-8) yields

$$\frac{T(Z)}{R(Z)} = \sum_{k=1}^{K} \frac{Z^{-1} H_k(Z)}{1 - Z^{-1} H_k(Z)} \qquad (2\text{-}12)$$

which may be combined with Equation (2-10) to give

$$G(Z) \triangleq \frac{R(Z)}{Y(Z)} = \frac{1}{1 + \sum_{k=1}^{K} \frac{Z^{-1} H_k(Z)}{1 - Z^{-1} H_k(Z)}} \qquad (2\text{-}13)$$

In the special case of a single operative module (which will be examined in what immediately follows) Equation (2-13) becomes

$$G(Z) = 1 - Z^{-1} H_1(Z). \qquad (2\text{-}14)$$

An estimator/predictor structure that has given excellent results is sketched in Figure 2-2. This modified bandpass filter may be used as the $H_r(Z)$ linear operator of Figure 2-1. Detections along the I and Q axes are performed at the filter radian center frequency ω_o and the resulting quadrature components are identically low-pass filtered. These recovered I and Q components remodulate carrier signals that are advanced in phase by $\omega_o T$, the carrier phase shift in one sampling period. The output signal $\theta(t)$ is an estimate of the spectral line signal as it will appear T-seconds in the future. Advantage is taken of the fact that the narrowband I and Q components of the spectral line will change negligibly during the sampling interval T and that only the carrier phase need be advanced to achieve good prediction. Since the sampling rates in this system must accomodate the total analysis bandwidth and since the spectral line widths are very small compared to the analysis bandwidth, the approximation involved here is a very good one.
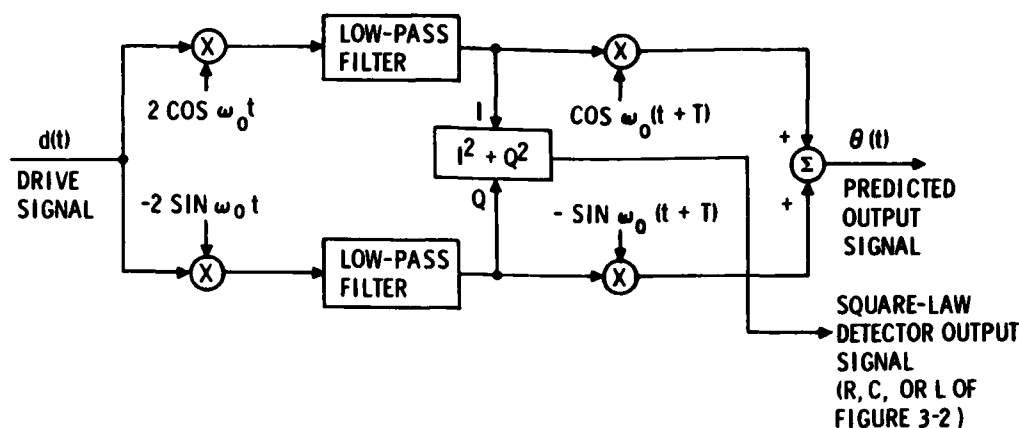
2-3

Figure 2-2. Estimator/Predictor Arrangement for Narrowband Signals

This linear operator is further simplified by specifying that the low-pass filters are single-pole filters of variable bandwidth. The input (x_n) and output (y_n) samples of the low-pass filters of Figure 2-2 satisfy

$$y_n = (1-\alpha) x_n + \alpha y_{n-1} \tag{2-15}$$

where the 3-dB cutoff frequency f_H is related to the parameter α by

$$\alpha \cong e^{-2\pi f_H T} \tag{2-16}$$

The 3-dB bandpass bandwidth of the Figure 2-2 filter is as a consequence $2f_H$.

The use of a simple single-pole filter in place of a more complicated structure may be defended for most applications without difficulty. The detailed spectral shape of the line signals is seldom known precisely so that "optimum" processing is not possible. Even if the power density spectrum were known with precision, a single-pole filter of appropriate bandwidth will usually perform so close to "optimum" that the difference is swamped by the errors inherent in the many other modeling assumptions made.

It is convenient at this point to consider "complex envelope" representations of the narrowband signals. The mathematical development of Equations (2-1) through (2-14) can apply to both real- and complex-envelope representations of signals if appropriate care is

taken. If the frequency term implied by $Z = \exp(j2\pi fT)$ is now measured from reference frequency $f_0(\omega_0 = 2\pi f_0)$, the transfer function of the processor of Figure 2-2 becomes

$$\frac{\theta(Z)}{D(Z)} = \frac{(1-\alpha)\,Z}{(Z-\alpha)} \; e^{+j\omega_0 T} \tag{2-17}$$

The additional delay of T seconds implied by the Z^{-1} operator of Figure 2-2 requires that the Z-transform of the complex envelope of the undelayed signal be multiplied by Z^{-1} and $e^{-j\omega_0 T}$ to account for carrier phase rotation. When this is done for Equation (2-17) and the result used in place of the $Z^{-1}H_1(Z)$ term of Equation (2-14), one obtains the RSA subsystem transfer function for a single-pole estimator/predictor based on a complex envelope signal representation. Using Equations (2-14) and (2-17) in this manner yields

$$G(Z) = 1 - \frac{(1-\alpha)}{Z-\alpha} = \frac{Z-1}{Z-\alpha} \tag{2-18}$$

The phase response from the input signal bus to the residual signal bus is shown in Figure 2-3. The phase is odd-symmetric about $f = 0$, hence there is a 180° jump in phase at $f = 0$. The frequency response curve from input signal bus to residual signal bus is also shown in Figure 2-3. A symmetric notch results with infinite attenuation at band center ($f = 0$). This implies that a pure CW signal would be perfectly predicted and thus entirely removed from the residual signal line. This represents neither much of a surprise nor much of an accomplishment. The behavior of this configuration for more realistic signal types will be examined in the next section. Note from Figure 2-3 that at the 3 dB frequencies of the single-pole filter an insertion loss of 3-dB in the G-function exists. This gives some indication of the "spillover" effects in the frequency domain of a tracker module of this type. At these frequencies the phase shift will be 45°.

The estimator/predictor operator discussed above forms one part of a particular tracker module configuration. The complete tracker module arrangement will be discussed in the next section along with a consideration of more realistic signal spectra.
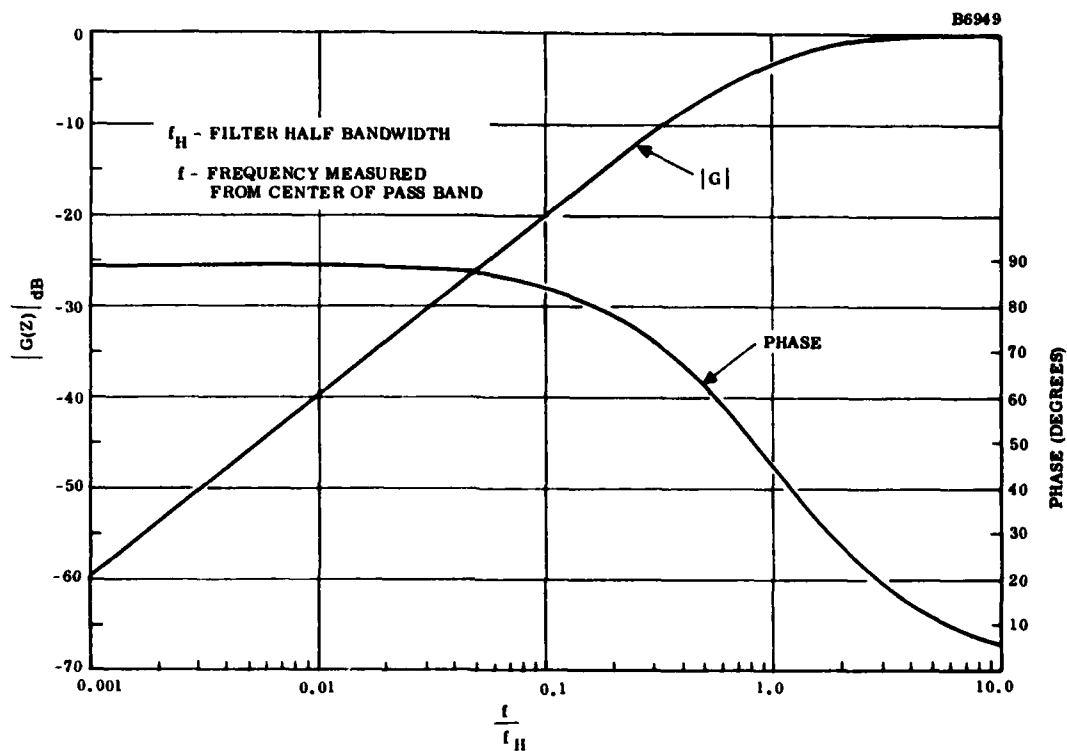
Figure 2-3. Residual Signal Line Response, $G(Z) = R(Z)/Y(Z)$, for Single-Pole Estimator/Predictor

SECTION III

TRACKER MODULE CONFIGURATIONS

The phase-lock loop arrangement of Figure 3-1 has been used with success as a tracker module in the context of Figure 1-1. In spite of the fact that both I and Q detections are made, this is not a Costas loop. It is a normal carrier-lock loop with the Q channel providing the error signal. The signal envelope is obtained from the I and Q signals and is used as a threshold against which the average component of I is tested. If the smoothed I signal is sufficiently close to the smoothed envelope value "lock" is declared and the logic line goes "true" and enables or closes switches S. The voltage controlled oscillator (VCO) signals are advanced in phase by $\omega_0 T$ and are remodulated by I and Q as shown to obtain the predicted output signal $\theta(t)$. The similarities between Figures 3-1 and 2-2 are clearly evident. However the operational philosophies from which these two figures are drawn are quite different. Figure 3-1 implies an actual phase lock to the signal with the temporal wanderings of signal phase being continually determined and followed. Figure 2-2 implies a filtering arrangement which expects that center frequency and bandwidth will be sensibly selected, but no demand is made with regard to phase coherence.
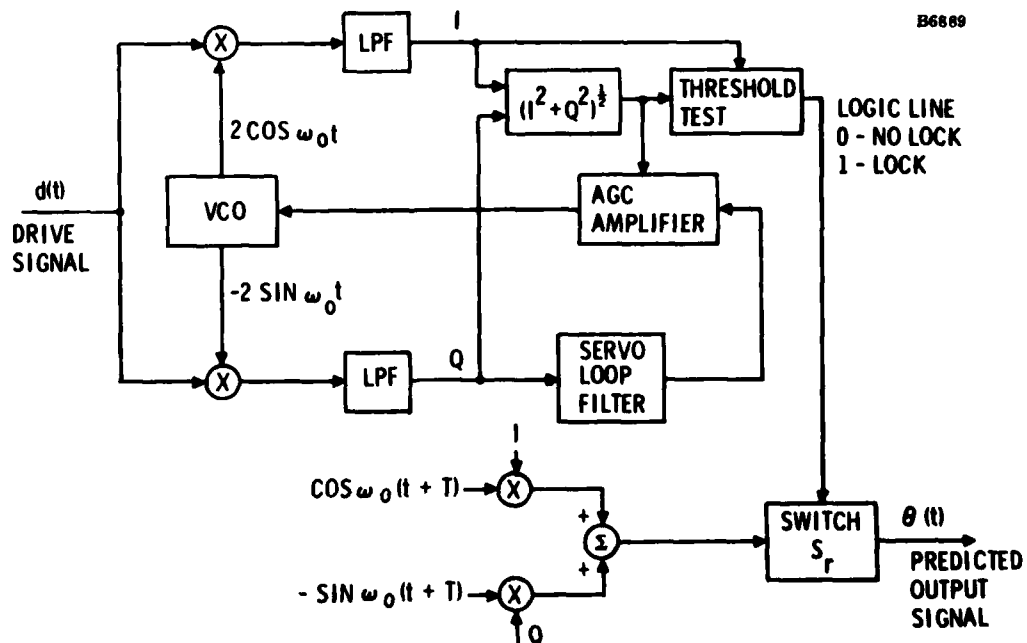

Figure 3-1. Phase-Lock Loop Tracker Module Arrangement

Figure 3-2 shows a three filter, frequency discriminator loop tracker module that has given very good results. The filter structures are of the type shown in Figure 2-2. The square-law detected outputs of the outboard filters are used to obtain a frequency tracking error signal through the computation of $(R - L)/R + L$. This error signal enters a filter frequency control unit which combines the direct error signal with its integral to produce a filter frequency (group) control signal, which is initialized by some means to represent the desired spectral line radian frequency ω_o. Offset control signals are also provided for the outboard filters as shown. In the examples of this paper the filter center frequencies are spaced by $2f_H$, the 3-dB single-pole passband bandwidth. When a frequency error occurs, the error signal causes the three filters to move together such that the center filter tracks the spectral line.
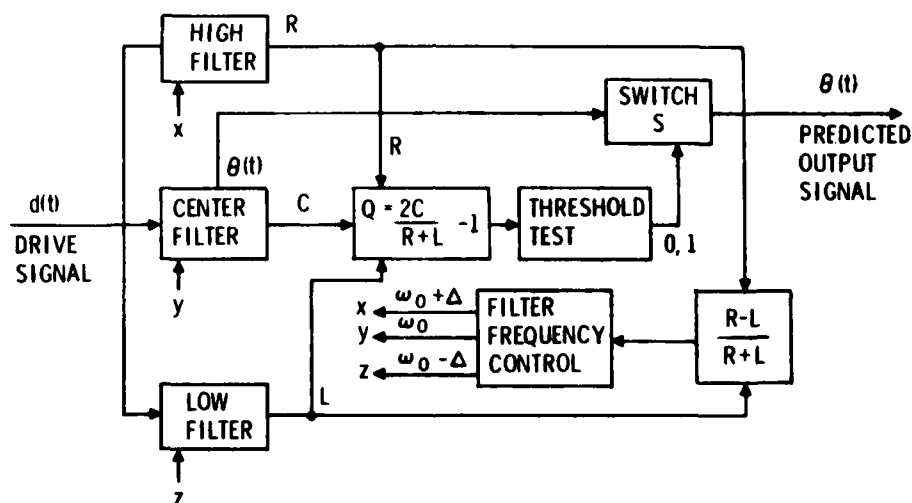
B6890

Figure 3-2. Frequency Discriminator Loop Tracker Module Arrangement

Track indication is derived from the Q-function calculation

$$Q = \frac{2C}{R+L} - 1 \qquad (3-1)$$

which displays an interesting and useful variation with filter bandwidth (kept the same for all three filters) for a given signal spectrum and background noise level. If the filter bandwidths are made very large compared to signal bandwidth, the output power levels of the filters (which is what the smoothed R, C, and L represent) approach equality. This occurs because background noise power tends eventually to dominate signal power as the filter bandwidths are increased. When this occurs the Q function of Equation (3-1) approaches zero.

3-2

At the other extreme consider filter bandwidths that are very narrow compared to signal bandwidth. The combined signal and noise spectrum is now essentially constant and equal in the response regions of the three filters so that the R, C, and L levels again become equal. This causes the Q function to tend once again toward zero. The Q function can be expected to have a peak value for some "optimum" filter bandwidth. The Q function is tested in the arrangement of Figure 3-2 in order to determine whether the "track" is true of false. If it is decided that a line is being tracked, switch S is closed and the predicted signal from the center filter (see Figure 2-2) is made available on an output line.

Both the phase-lock loop (PLL) tracker module of Figure 3-1 and the frequency discriminator loop (FDL) tracker module of Figure 3-2 have been used satisfactorily. The choice between these two-tracker module types will depend on many factors including the specific application at hand. The FDL tracker is chosen for further analysis in this paper for several reasons. Very weak lines can be tracked using the FDL by long-term smoothing of R, C, and L which cannot be handled at all by the PLL tracker. This is because the temporal behavior of the I and Q components are completely masked by noise. Even at higher signal levels the signal envelope fluctuations and the attendant phase discontinuities that accompany a fade, cause annoying and recurring losses of lock in the PLL case. Since acquisition is always more difficult than tracking, the repeated supervisory demands on the Tracker Control Unit (Figure 1-1) because of PLL dropouts becomes a burden. In certain signal-to-noise ratio (SNR) regimes the PLL may give somewhat better estimates of signal frequency and phase, however these quantities are certainly available from the FDL. Note in Figure 2-2 that an arctangent operation on the smoothed I and Q components will yield signal phase. It should also be remembered that a linear bandpass filter with an intelligently-selected bandwidth provides spectral line signal estimation performance which is, by any practical measure, at the "optimum" performance level.

With regard to the FDL tracker module a means for selecting bandwidth will now be considered. For RSA purposes estimation and prediction performance are essentially one and the same due to the high ratio of sampling rate to signal bandwidth as previously discussed.

For the single-pole filter of Equation (2-15) if Z-transforms are taken and the usual narrowband approximations are made, the filter transfer function may be represented by

$$H(f) \approx \frac{1}{1 + j\left(\frac{f}{f_H}\right)} \tag{3-2}$$

where f is measured from band center and f_H is one-half the total bandpass 3-dB bandwidth. For convenience in discussion let the spectral line signal have a (two-sided) power density spectrum of unity over a bandwidth of B Hz. The signal to noise ratio will be indicated by γ.

If the mean-square error ϕ is taken as the measure of the goodness of signal estimation, then by the usual calculus one obtains:

$$\frac{\phi}{B} = 2 - \frac{2f_H}{B}\left[2\tan^{-1}\left(\frac{B}{2f_H}\right) - \frac{\pi}{\gamma} \right] \qquad (3\text{-}3)$$

The results are shown in Figure 3-3. The filter bandwidth required for best estimation varies with SNR. Two types of errors exist: noise and signal distortion. Increasing bandwidth increases noise but lowers signal distortion. The optimum bandwidth increases with increasing SNR.

It will now be shown that the filter bandwidth which maximizes the Q-function (a readily measurable quantity) will also result in near-optimum estimation performance. As before, the signal spectrum is assumed to have a (two-sided) unit power density spectrum over a passband bandwidth of B Hz. The three single-pole filters have a bandwidth of $2f_H$ and a center frequency spacing of $2f_H$. Letting $x \overset{\Delta}{=} f_H/B$, $\gamma = $ SNR, routine analysis yields

$$Q = \frac{2\tan^{-1}(1/2\,x) + \pi/\gamma}{\tan^{-1}\left[\dfrac{1/x}{5 - (1/2x)^2}\right] + \dfrac{\pi}{\gamma}} - 1 \qquad (3\text{-}4)$$

The results are shown plotted in Figure 3-4. Comparing Figures 3-3 and 3-4 shows that a bandwidth adjustment for maximum Q yields nearly optimum estimation performance. While this simple analysis has idealized the signal spectrum and used mean-square error as the performance measure, practical experience has indicated that adapting to peak Q-values is indeed a viable strategy.

As a practical matter parameter optimization has not proved to be a critical problem. The performance curves in the real world appear to have broad, smooth peaks. Furthermore, the nonstationary nature of most signals and noises encountered makes precise performance peaks very difficult to find and verify in any event.
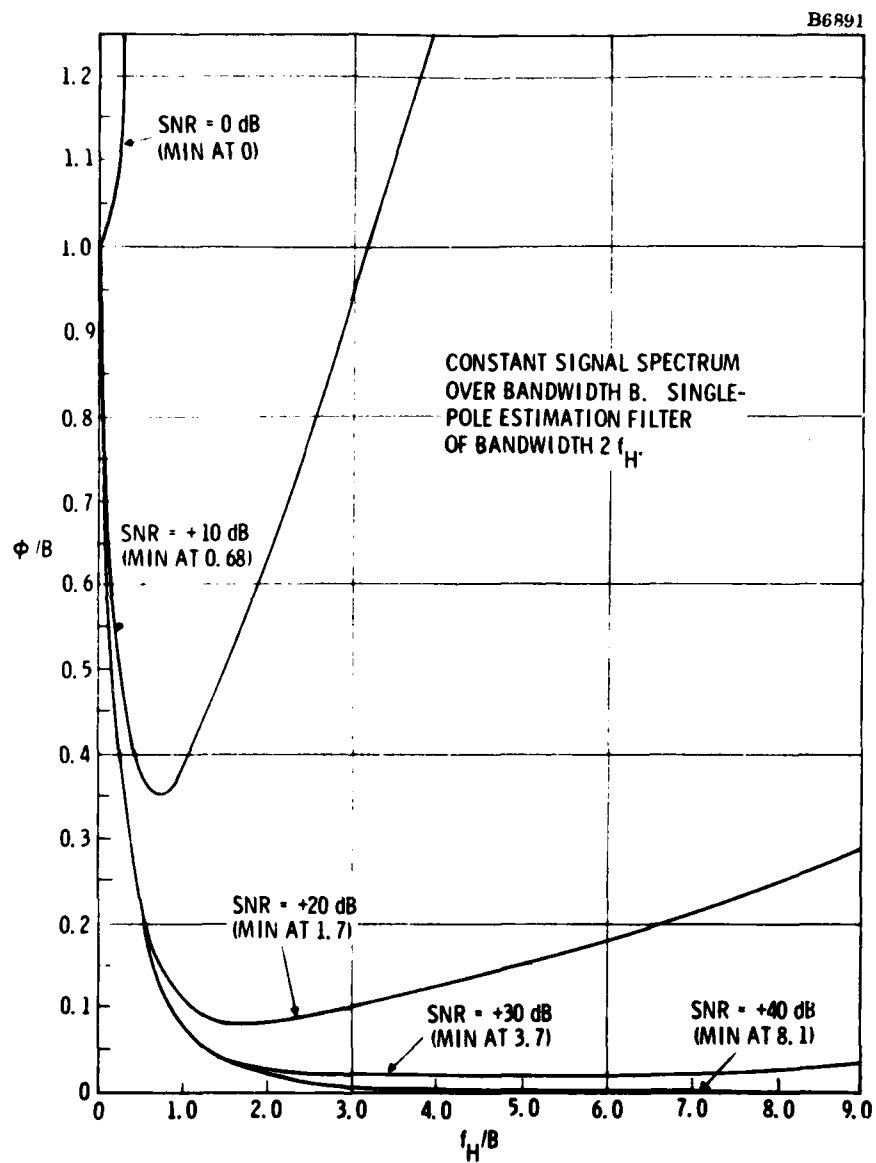
3-4

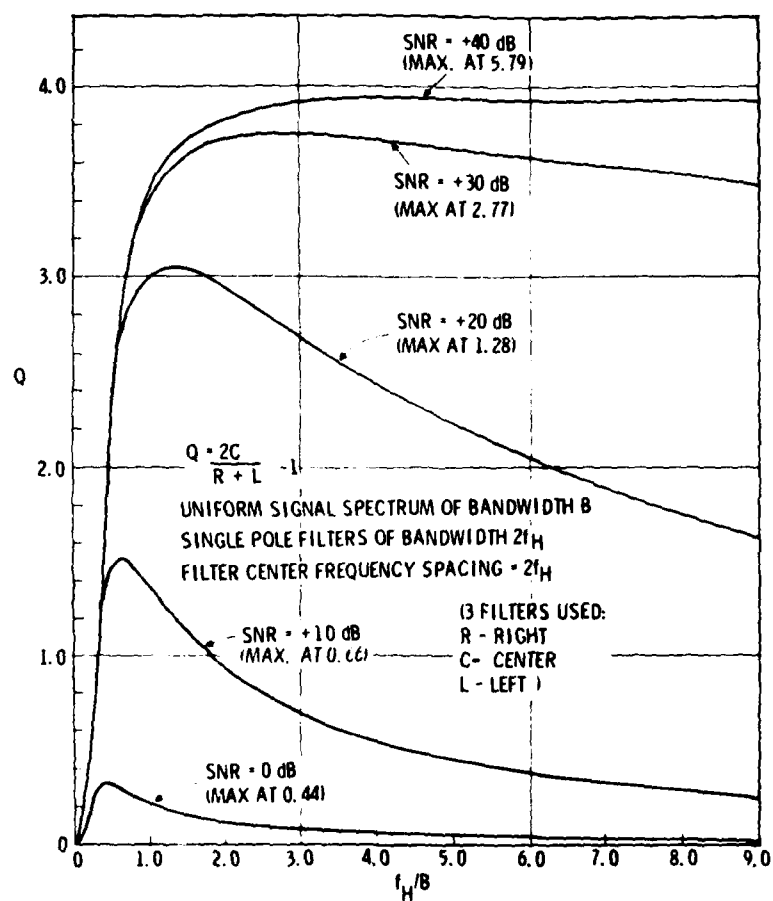Figure 3-3. FDL Tracker Normalized Mean-Square Error of Signal Estimate vs f_H/B

Figure 3-4. Frequency Discriminator Loop Tracker Module Q Parameter vs f_H/B

SECTION IV

SEA TEST EXAMPLES

The data processed in the examples which follow was obtained from completely unclass-
ified sources. The test scenario involved transmission from one vessel of four highly stable
and coherent spectral lines at 187 Hz, 195 Hz, 200 Hz, and 206 Hz ("projector lines"). A
broadband noise signal was also radiated by the transmit vessel. These signals were re-
corded aboard another vessel. When the recordings were analyzed a fifth line was discovered
near 215 Hz. This line was found to be generated by a pump aboard the receive vessel and is
described in what follows as a "pump line".

The transit of one vessel past the other during the test caused the four projector lines
to display a doppler-time history pattern of interest. The task of the RSA processor sub-
system involved accurate measurement of this Doppler-time history for the four projector
lines. In addition it was required that all lines (including the pump line) be removed to pro-
vide access to the broadband noise signal which was also radiated by the transmit vessel.
This broadband signal, unencumbered by narrowband line "interference", was to be delivered
to a post-processing subsystem connected to the Residual Signal Bus (Figure 1-1). In the
following the frequency measurement and then the line-removal performance of the RSA sub-
system will be discussed.

In Figure 4-1 plots are shown of the measured projector line frequencies. This data
is taken from computer listings which contained the measured frequencies listed to the near-
est millihertz. Measurements were printed every 5s and the time span of the data of Figure
4-1 was chosen to include the closest point of approach (CPA) of the two vessels which occur-
red at a range of about 4000 yards. The filter bandwidths for the four modules assigned to
the projector lines were 100 mHz. A fifth module was assigned to the pump line at 215 Hz
with a filter bandwidth of 1 Hz. This last tracker was assigned for line-elimination purposes
only, the frequency data from this module was ignored.

An estimate of the quality of the frequency measurements of Figure 4-1 was obtained
by the process to be described. If the transmit frequency for line n is represented by F_{Tn}
and the received frequency by F_{Rn}, then

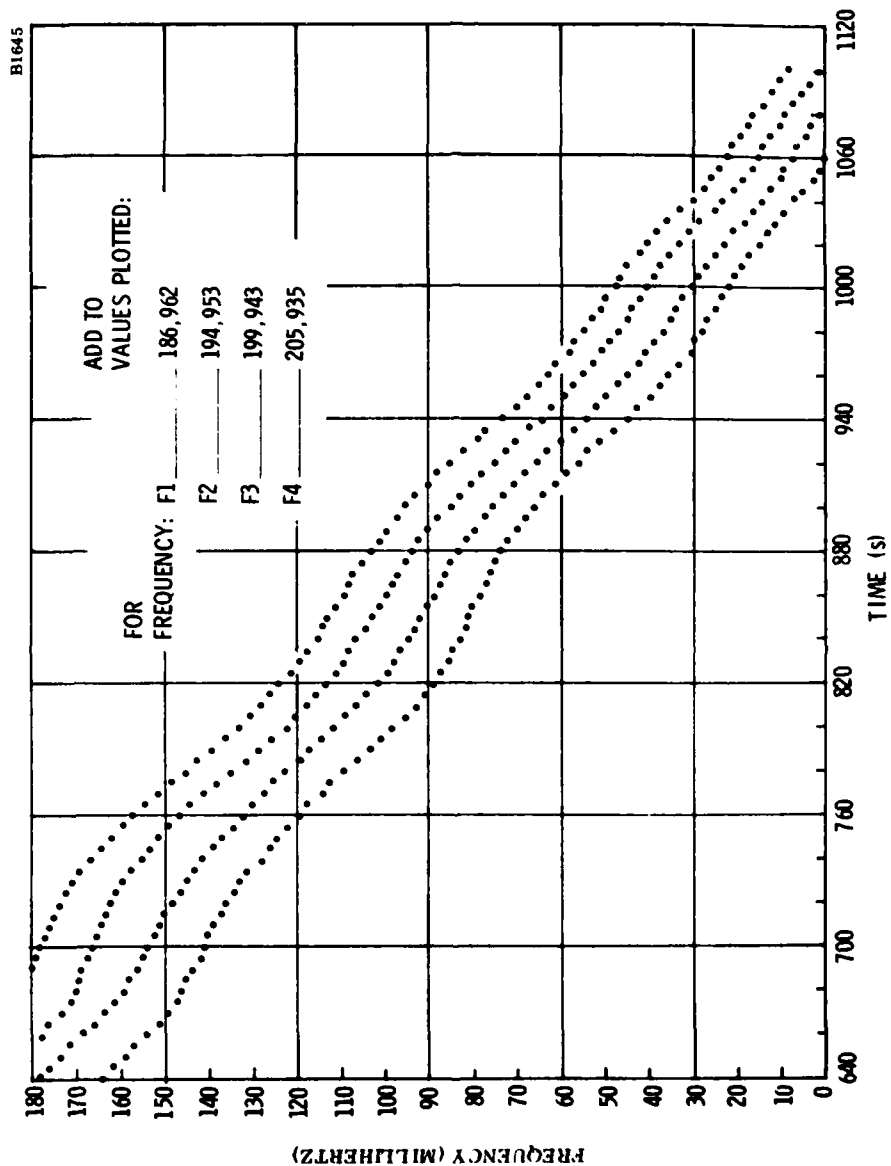$$F_{Rn} = F_{Tn} \left(1 + \frac{v}{c}\right) \qquad (4-1)$$

Figure 4-1. Measured Received Frequency of Four Projector Lines (mHz)

4-2

where v is the relative closing velocity between the two vessels and c is the sound velocity in the medium. One line may be used as a reference (line 2 in this case) to obtain a $(1 + v/c)$ value using Equation (4-1). The other line frequencies may then be predicted from this value using the known transmit frequencies. Let E_n represent the error between the predicted frequency and the measured frequency. Then

$$E_n = \frac{F_{Tn}}{F_{T2}} \, F'_{R2} - F'_{Rn} \, , \quad n = 1, 3, 4 \tag{4-2}$$

where F'_{R2} and F'_{Rn} are the measured received frequencies.

If the received frequency measurements are assumed to be unbiased, these measurements may be represented by

$$F'_{Rn} = F_{Rn} + \delta_n \, , \quad n = 1, 3, 4 \tag{4-3}$$

where F_{Rn} represents the true signal frequency at the receiver and δ_n represents a zero-mean error term in the measurement. Equation (4-2) may be rewritten as

$$E_n = \frac{F_{Tn}}{F_{T2}} \left(F_{R2} + \delta_2 \right) - \left(F_{Rn} + \delta_n \right) \, , \quad n = 1, 3, 4 \, . \tag{4-4}$$

However, since

$$\frac{F_{R2}}{F_{T2}} \, F_{Tn} = \left(1 + \frac{v}{c} \right) F_{Tn} = F_{Rn} \, , \quad n = 1, 3, 4 \tag{4-5}$$

then

$$E_n = \left(\frac{F_{Tn}}{F_{T2}} \right) \delta_2 - \delta_n \, , \quad n = 1, 3, 4 \tag{4-6}$$

The error quantities E_n should therefore have zero mean. As measured for the run of Figure 4-1, there resulted $\bar{E}_1 = -0.05$, $\bar{E}_3 = +0.18$, and $\bar{E}_4 = -0.30$ mHz, giving an overall average of -0.06 mHz. At time 955 in this run the measured frequencies as listed were exactly 187.000, 195.000, 200.000 and 206.000 Hz. These are precisely the synthesized transmit frequencies. Since this time lies within the exercise track reconstruction CPA window, we have further evidence that the frequency measurements produced by the RSA modules are unbiased.

If the measurement error terms δ are assumed to be independent, zero mean and have the same mean-squared value σ_δ^2, squaring both sides of Equation (4-6) and averaging yields

$$\sigma_\delta^2 = \frac{\overline{\left(E_n\right)^2}}{1+\left(\dfrac{F_{Tn}}{F_{T2}}\right)^2} \quad , \qquad n = 1, 3, 4 \tag{4-7}$$

The three values of $\overline{\left(E_n^{\,2}\right)}$ of the Figure 4-1 data were 0.66, 1.46, and 1.21 which yields σ_δ^2 values of 0.34, 0.71, and 0.57. Averaging these results gives a σ_δ of 0.73 mHz.

These results indicate that the frequency measurements for the run of Figure 4-1 are essentially unbiased and have a standard deviation of the order of three-quarters of one millihertz.

Figure 4-2 shows a spectrogram of the RSA output (Residual Signal Bus) signal with one operative tracker module assigned to the pump line at 215 Hz. As a consequence this line does not appear in Figure 4-2, however the four projector lines are clearly visible at 187, 195, 200 and 206 Hz. The broadband noise signal radiated by the transmit vessel extends from about 100 Hz to 500 Hz and the noise background peak in the vicinity of 150 Hz is believed to arise from hull noise at the receive vessel.

Figure 4-3 shows a spectrogram of the RSA signal output when five trackers are deployed, one for each of the projector lines and one for the pump line. (Plot normalization results in a +5.4 dB shift of Figure 4-3 data relative to that of Figure 4-2.) As may be seen, all five dominant lines have been suppressed so that background noise and other narrowband components now dominate the spectral plot. In these last two figures an (FFT) window of one second was used and five FFT outputs were averaged to produce the data shown. The time periods from which the data were drawn were about 2.5 minutes apart.

A different perspective on frequency-domain effects may be obtained from the lofar-grams shown in Figures 4-4 to 4-6. The first of these amplitude versus frequency time-history displays, Figure 4-4, shows the RSA input signal. The five lines dominate the display as expected. Figure 4-5 shows the RSA output signal when five trackers are deployed. The background noise peak in the 150 Hz neighborhood now saturates the display as the five line levels have been significantly reduced. Vestiges of the four projector lines may still be seen in Figure 4-5 even through their level appears to be reduced below that of the back-ground noise peak near 150 Hz. Note that the pump line (compare with Figure 4-4) has been reduced to a broad smear in Figure 4-5. This pump line is much more typical of real-world lines than the projector lines, of course.
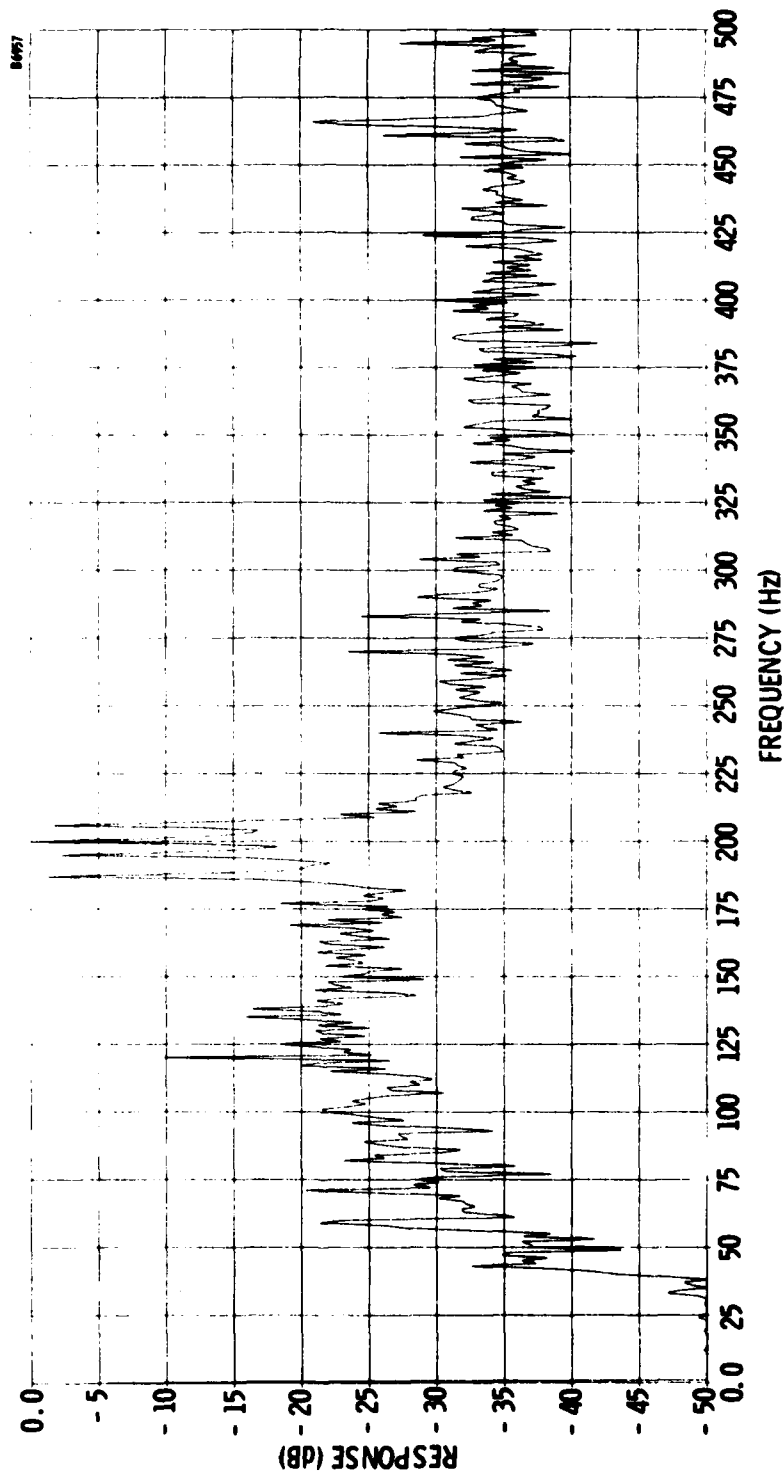
4-4

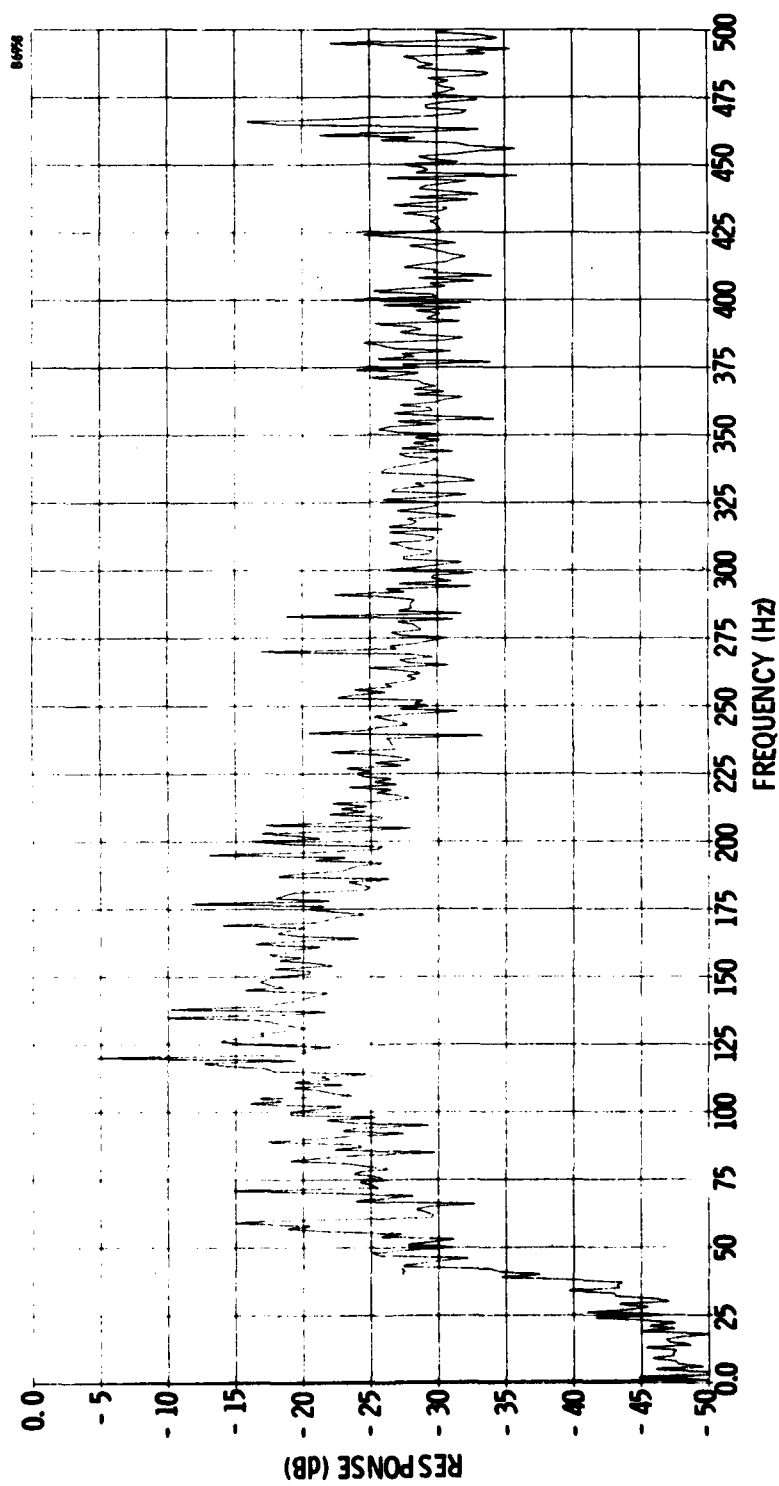Figure 4-2. Spectrogram of RSA Output Signal, One Operative Tracker at 215 Hz (Pump Line)

4-5

Figure 4-3. Spectrogram of RSA Output Signal, Five Operative Trackers at 187, 195, 200, 206 and 215 Hz
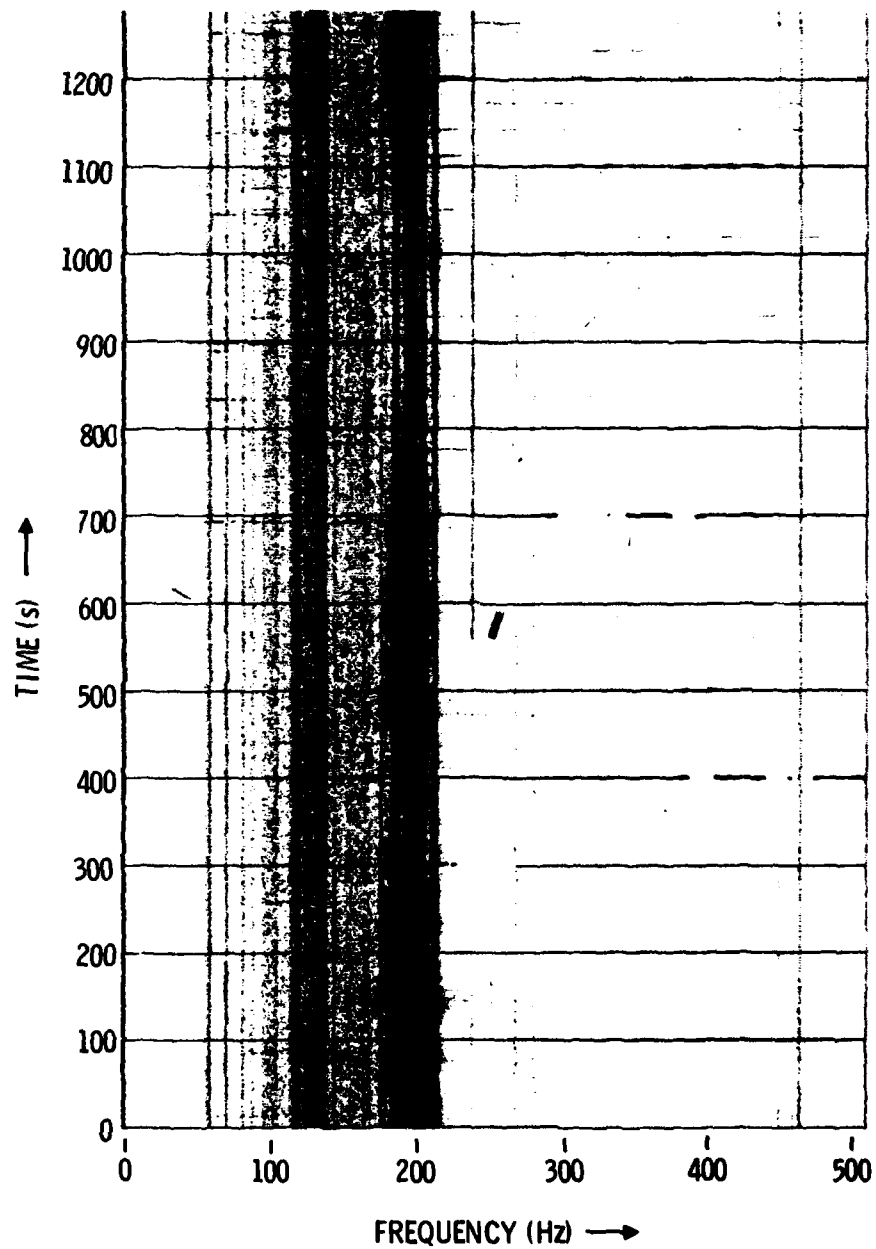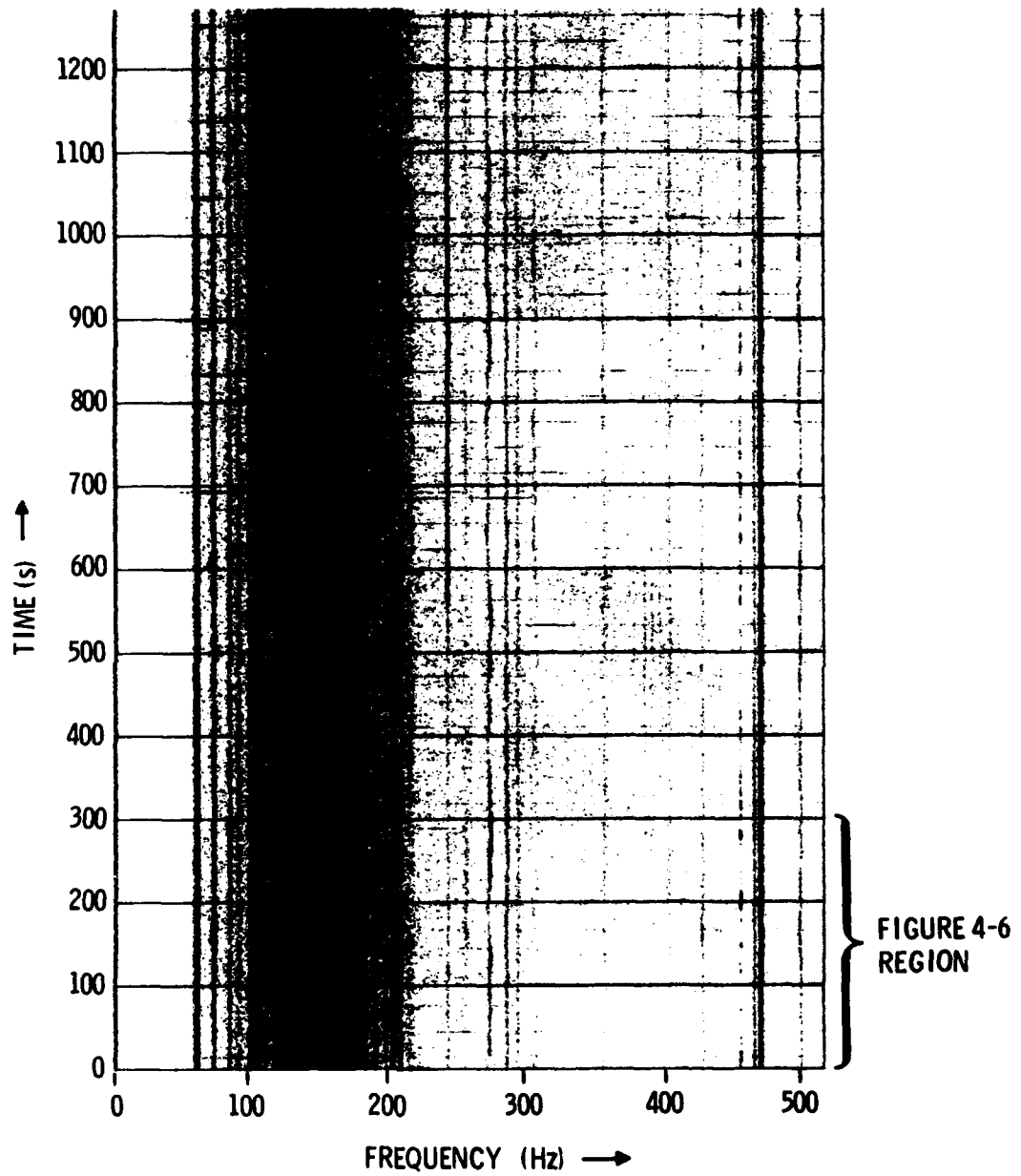
Figure 4-4. Lofargram of RSA Input Signal

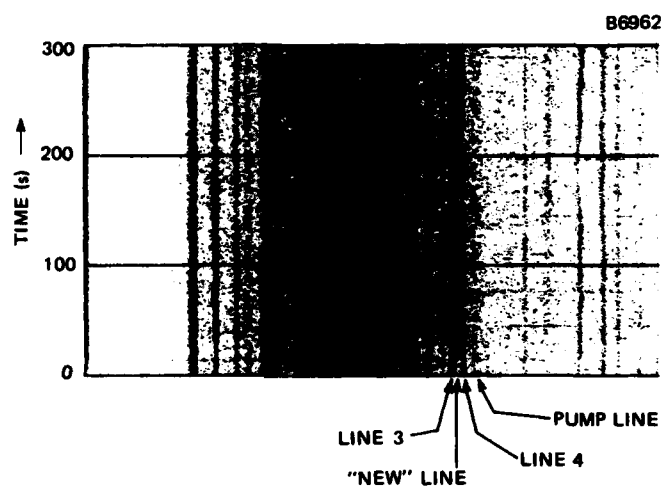Figure 4-5. Lofargram of RSA Output Signal with Five Trackers Deployed

Figure 4-6. Enlarged View of Early Figure 4-5 Data Showing New Line Between Projector Lines 3 and 4

(The strength, source purity and short water path of the projector lines create some unusual problems in the demonstration of the RSA technique. Estimation module bandwidths of 100 mHz were used for the frequency measurements of Figure 4-1. This yields excellent frequency estimation but poor line elimination performance. The spectrograms of Figures 4-2 and 4-3 and the lofargrams of Figures 4-5 and 4-6 were obtained using 1 Hz filter bandwidths. This gave much better suppression but higher variance frequency data. Wider filter bandwidths could have been used to obtain much more impressive line suppression performance for the lofargrams. It is strongly indicated that energy arrival at the receive vessel contains two components. A carrier component is present whose average frequency is truly responsive to radial platform velocity. Water path phase and amplitude modulation effects create sideband energy as a second received component which is at a non-trivial level relative to background noise due to the very high projector line levels. This creates the unusual condition in which poor suppression accompanies good frequency estimation. This rather artificial situation may have much more scientific value as regards medium-effects studies using RSA than engineering utility.)

Of special interest in Figure 4-5 is the new line now visible between projector lines 3 and 4. An enlargement of this region of Figure 4-5 is shown in Figure 4-6. The dynamic range reduction provided by the RSA subsystem allows much more low-level data to be investigated using limited dynamic range displays as evidenced by Figure 4-6. While these projector lines are atypical, the enhanced capability of the lofargram display when operated in conjunction with an RSA subsystem is a routine and very useful benefit. The "new" line uncovered in Figures 4-5 and 4-6 stays between projector lines 3 and 4 for the entire run. The etiology of this spectral component is not understood at this time.

The sea data processed here was readily available and its use was convenient for demonstration of the RSA technique. The highly accurate measurements of frequency obtained were made possible by the unusual quality of the source of the projector lines and by the short water path involved in acoustic propagation. In most real-world situations, conditions are not as fortuitous as those found here, of course, and somewhat more uncertainty in frequency estimation is inevitable. Since individual tracker module parameters may be tailored to the specific characteristic of the assigned line, frequency measurement may be optimized for each line of interest. The absolute level of optimized frequency estimation will vary considerable from line to line depending upon spectral purity, signal-to-noise ratio, and center frequency temporal behavior (line dynamics).

SECTION V

CONCLUSIONS

The residual signal analysis technique represents a unique and unusual approach to the line tracking problem. Because of its novelty and the limited resources committed thus far to its development, much more work remains to be done in order to exploit the inherent advantages of the concept.

ENGLISH-METRIC/METRIC-ENGLISH CONVERSION TABLE

mm	=	0.1 cm	lb	=	453.6 g
cm	=	0.3937 in.	lb	=	0.4536 kg
cm	=	0.0328 ft	metric ton	=	1.12 tons (U.S.)
cm	=	10 mm	m	=	39.37 in.
cm^2	=	0.1550 in.^{2}	m	=	3.281 ft
cm^2	=	$1.076 \cdot 10^{-3}$ ft^2	m	=	1.0936 yd
cm^3	=	0.061 in.^{3}	m^2	=	10.76 ft^2
cm^3	=	$3.531 \cdot 10^{-5}$ ft^3	m^2	=	1.196 yd^2
ft	=	30.48 cm	m^3	=	35.32 ft^3
ft	=	0.3048 m	m^3	=	1.430 yd^3
ft^2	=	0.0929 m^2	mi	=	1.6093 km
ft^2	=	929.37 cm^2	mi	=	5280 ft
ft^2	=	$9.294 \cdot 10^{-3}$ km^2	mi	=	0.87 nmi
ft^3	=	0.0283 m^3	mi	=	1760 yd
in.	=	2.54 cm	mi^2	=	2.59 km^2
in.^{2}	=	6.452 cm^2	mi/h	=	0.87 knots
in.^{3}	=	16.387 cm^2	nmi	=	1.852 km
μm (micron)	=	0.001 mm	nmi	=	6076 ft
μm	=	10^{-6}m	nmi	=	1.15 mi
μm	=	10^{-4} cm	yd	=	0.9144 m
μin.	=	$2.54 \cdot 10^{-5}$mm	yd^2	=	0.836 m^2
kg	=	2.2046 lbs	yd^3	=	0.7645 m^3
km	=	3281 ft	qt	=	0.946 liter
km	=	0.6214 mi	liter	=	1.057 qt
km	=	0.55 nmi	acre	=	43,560 ft^2
km^2	=	$1.076 \cdot 10^7$ ft^2	acre	=	4046.72 m^2
km^2	=	0.381 mi^2	rad	=	57.2958°
km/h	=	0.913 ft/s	deg	=	0.017 rad
knot	=	1.152 mi/h	°F	=	9/5(°C) + 32
oz	=	28.35 g	°C	=	5/9(F° − 32)
oz	=	0.062 lbs			